CHAPTER 1

INTRODUCTION AND LITERATURE REVIEW

1.1. Introduction

The demonstration of Vacuum Electron Devices (VEDs) were first made in 1883, when Thomas Edison measured an electric current from a heated filament cathode to a positively- biased plate, or anode, in an evacuated bulb [Sobol *et al.* (1984)]. By exploiting this property Fleming developed a valve (diode) in 1904 which was used for detection of DC current. Later in 1906, Lee defrost introduced a grid to the Fleming's valve and developed a triode. These glass vacuum tubes were employed for the radio communication until the magnetron was invented [Collins *et al.* (1948)] that generates significant microwave radiation. The advent of World War II further served as a catalyst for the development of microwave tubes. The need for high power microwave signals used for radar detection systems brought about the 3GHz, 10kW magnetron in 1939 [Boot *et al.* (1946)], and the klystron, invented by the Varian brothers in 1937 [Bryant *et al.* (1886)].

Ever since then, microwave tube community has been rapidly advancing due to an ever increasing demand for higher powers, greater efficiency, and higher frequencies. New and varied applications for these devices have allowed the industry to evolve and thrive. Many nuclear fusion experiments require gyrotrons to provide high power microwaves over long pulses for heating plasmas to very high temperatures, as will be discussed. The proposed International Thermonuclear Experimental Reactor (ITER) will require many of these gyrotrons producing powers which have never been reached before. Gyrotrons are also being seriously considered for imaging in medical applications, such as Electron Paramagnetic Resonance (EPR) used in Dynamic Nuclear Polarization (DNP) spectroscopy. At MIT, a 250 GHz gyrotron has been demonstrated for use in DNP [Bajaj *et al.* (2003)], and a 460 GHz second-harmonic gyrotron is being developed to provide greater resolution [Hornstein *et al.* (2006)].

Microwaves are serving our society in almost every prospect of day-to-day life. Their use is omnipresent, from ground base to the deep space communications, for civilian as well as defence requirements, space exploration, scientific researches to medical applications, strategic to industrial applications, generation of thermonuclear energy, and so on [Amboss *et al.* (1980), Andronov *et al.* (1978), Barker *et al.* (2001), Chatterjee *et al.* (1999), Chu *et al.* (1978), Collin (1966), Curie (1989), Gandhi (1981), Gaponov *et al.* (1994), Gilmour (1986), Hirshfield *et al.* (1977), Liao (1988), Singh *et al.* (2011)]. With increasing demand of device operation at higher frequencies for new applications, the research are now pushed towards the development of millimeter and sub-millimeter wave sources [Chatterjee (1999), Chu (2004), Edgcombe (1993), Emerson (1997), Felch *et al.* (1999), Gaponov *et al.* (1994), Kartikeyan (2004), Nusinovich (2004)]. At these frequencies, microwave tubes (vacuum electron beam devices) are only capable to deliver high power at which their solid-state counterparts are not able to compete [Chu (2004), Kartikeyan *et al.* (2004), Liao (1988)].

The microwave tubes find its applications over wide range of areas, such as, communication systems, radars, electronic warfare weaponry, plasma heating in fusion research, material processing, medical imaging, advanced particle accelerators, and many more [Chu (2004), Gold *et al.* (1997), Kartikeyan *et al.* (2004), Smith *et al.* (1993), Thumm (1996)]. These applications span over variety of technologies, such as, ground base point-to-point communication, satellite communication, satellite-to-home communication, thermal reactors (heating of hydrogen isotopes at ignition temperature), military radars (missile tracking and guidance), civilian radars (remote sensing, weather detection, highway collision avoidance, airport traffic control, speed detectors, air-traffic control, mapping of ground terrain), medical applications (hyperthermia, lung water detection, monitoring of heartbeat), etc. Moreover, microwave tubes operating in millimeter wave extends its applications including high resolution radar and high information density communication, deep space and specialized satellite communication, advanced high gradient RF linear particle accelerators in high energy physics, plasma diagnostics and chemistry, waste remediation, laser pumping, electron cyclotron resonance (ECR) heating of fusion plasmas, radar and imaging in atmospheric and planetary science, nonlinear spectroscopy, high power microwaves (HPM) electronic warfare, etc. [Barker *et al.* (2004), Benford (1992), Chu (2004), Feinstein *et al.* (1987), Felch *et al.* (1999), Flyagin *et al.* (1988), Gold *et al.* (1997), Grantstein *et al.* (1987), Kartikeyan *et al.* (2004), Nusinovich (2004), Sakmoto (2006), Singh *et al.* (2011), Thumm (2002, 2003, 2010)].

The broad sweep of progress in RF vacuum electronics across a variety of devices was proposed in terms of the evolution of a "power density" as a figure of merit by Nergaard in 1960 providing an insightful basis for comparing device types [Parker *et al.* (2002)]. The physical significance derives from the fact that the maximum beam or charge carrier power that can be transported through a device is proportional to the cross-sectional area of the circuit, i.e., inversely proportional to the operating frequency. As operating frequency increases, the power handling capacity of device reduces. These necessities along with the development of superconducting magnet gave birth to a new class of microwave devices, i.e., the fast wave devices. The fast wave devices includes gyromonotron, gyro-traveling-wave tube (gyro-TWT), gyroklystron, gyro-BWO, and gyrotwystron [Baird (1979), Chu (2004), Felch (1999), Nusinovich (2004)].

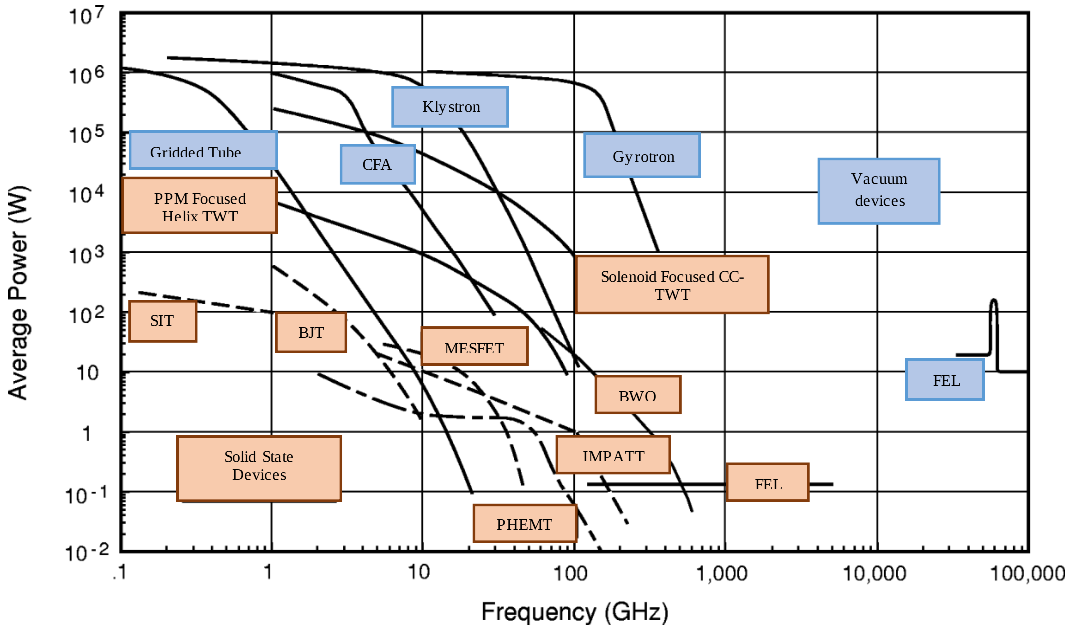

Figure 1.1: Comparison of average power versus frequency for various types of devices.

The gyro-devices and FEL surpassed the conventional slow-wave devices in the mid-1970 for high power at millimeter and sub-millimeter wave frequency range. A typical comparison of average power delivered by different devices has been represented in Fig. 1.1. In fact, microwave tubes faced stiff competition from their solid state counterpart at some stage since the later was based on the highly developed semiconductor technology. Afterwards around seventies the technology would be replaced by the semiconductor technology. However, the scenario has been changed in eighties with the growth of the microwave tubes in terms of the performance [Baird *et al.* (1979), Symons *et al.* (1986), Kartikeyan *et al.* (2004), Nusinovich (2004), Thumm (2010)]. Since, only microwave devices are capable to produce thousand times or more output power at higher frequency regime compared to the semiconductor based devices. Miniaturised size of semiconductor devices at higher frequencies limits the power handling capability whereas in case of vacuum devices, size restriction is not an issue at the higher frequencies and they can deliver high output power with considerable power handling capability [Kartikeyan *et al.* (2004), Nusinovich (2004)].

1.2. Fast-Wave Gyro-Devices

The performance of quantum-mechanical devices, like, laser degrades in terms of average output power level with decreasing frequencies and that of conventional microwave tubes with increasing the frequencies of operation [Edgcombe (1993), Gilmour (1986), Nusinovich (2004), Thumm *et al.* (2005)]. These results a technological gap in the millimeter-wave ranges to achieve substantial device performances. This happens due to the reduction in energy of each quantum with the frequency and simultaneously it is difficult to retain the population inversion in a quantum-mechanical device. On the other hand, with increase in the operating frequencies, transverse dimension of microwave devices shrinks rapidly, thereby reducing the power handling capability. Hence, with increasing operating frequency of conventional microwave tubes, the RF output power decreases due to the various limiting factors arise such as DC power dissipation, RF losses, electron current density, material breakdown, etc. This has motivated the search for the new electron beam devices that fulfills the gap in terms of appreciable power level in the microwave and millimeter wave regions, for instance, gyrotron devices based on cyclotron resonance maser (CRM) instability [Baird (1979), Barker (2001), Basu (1996), Edgcombe (1993), Felch *et al.* (1999), Gilmour (1986), Nusinovich (2004)].

In gyro-devices, a hollow gyrating electron beam interacts with the transverse electric mode supported by a fast-wave-guiding structure, like, a cylindrical waveguide or cavity. In these devices, basically the electron beam is made periodic rather than the interaction structure that supports a fast waves. In a gyrotron, transverse kinetic energy of electrons is converted into electromagnetic energy rather than axial kinetic energy (as in a TWT) or potential energy (as in a magnetron) during the beam-wave interaction mechanism. The Doppler-shifted frequency is made nearly equal to the cyclotron frequency or any of its harmonics for the cyclotron resonance takes place, unlike in a device like TWT where the electron DC beam velocity is made synchronous with the RF phase velocity.

Similar to the slow-wave devices, transverse dimension of the interaction structure of fast-wave devices also decreases with the increase of frequency. However, in gyrotron device operation at the higher-order modes lead to a further increase in the waveguide transverse dimension [Kartikeyan *et al.* (2004), Liu (2000), Nusinovich (1999)]. This increase in transverse dimension of the interaction structure reduces the power loss density at the cavity or waveguide wall of the devices. Another advantage of a fast-wave gyro-device structure is that the electron beam can be placed far from the interaction structure wall to realize larger interaction field. This also reduces the problem of beam interception caused by the metallic boundaries.

The fast-wave gyro-devices, e.g., gyrotron are based on CRM instability and electrons bunching is relativistic. The electron bunches are kept in the decelerating RF phase which yields that most of the electrons interacting with RF waves transfer their energy to RF instead of taking energy from the later. This can be obtained by slightly detuning the cyclotron resonance condition while in a slow-wave device, this is done by slightly offsetting the synchronism between the DC beam velocity and RF phase velocity [Basu (1996), Edgcombe (1993), Gilmour (1986), Kartikeyan *et al.* (2004)]. Further the classification of gyrotron devices are done on the basis of their interaction mechanism. The synchronism between beam mode line and waveguide mode curve for beam-wave interaction of different gyrotron devices are discussed through the dispersion curve in Section 1.2.1.

1.2.1 Dispersion relation

The operational characteristic of the device is governed by the dispersion relation and device synchronism condition can be obtained at the grazing intersection between the beam mode and waveguide mode dispersion curve. In a gyrotron device, the condition of synchronism between the fast cyclotron wave and electron beam motion, transverse to a DC magnetic field, leads to a beam-mode dispersion relation of a gyro-device as described below [Basu (1996), Chu (2004), Edgcombe (1993), Gaponov-Grekhov *et al.* (1994), Gilmour (1986), Kartikeyan *et al.* (2004), Nusinovich (2004), Thumm (2010)].

1.2.1a Beam-mode dispersion relation

The beam mode dispersion relation can be obtained using the concept that over a cyclotron period, one or more RF cycles are completed [Basu (1996)]. Considering a gyrating electron beam that completes its one gyration in time T_c. The RF phase of the electric field component can be given as $\omega t-\beta z$ where ω is the wave frequency, β the propagation constant or wavenumber. After one gyration time period, the initial phase will change and can be given as $\omega(t+T_c)-\beta(z+v_zT_c)=\omega t+\omega T_c-\beta z-\beta v_zT_c$, where s is the beam mode or harmonic number, and v_z is axial beam velocity. Now, putting $s(2\pi)=(\omega-\beta v_z)T_c$, the initial phase change can be written as $\omega t-\beta z+s(2\pi)$. Considering,

$$s(2\pi)=(\omega-\beta v_z)T_c \tag{1.1}$$

$$s(2\pi)/T_c=\omega-\beta v_z\ . \tag{1.2}$$

The cyclotron frequency is $\omega_c=2\pi/T_c$, so (1.2) can be written as

$$s\,\omega_c=\omega-\beta v_z \tag{1.3}$$

$$\omega - \beta v_z - s\,\omega_c = 0 \quad , \tag{1.4}$$

where,
$$\omega_c = eB_0 / m_e \tag{1.5}$$

B_0 is the axial DC magnetic field, e and m_e are the magnitude of electron charge and mass at the rest, respectively. Since, gyro-devices are relativistic devices, so including relativistic mass factor (γ) into equation (1.4), it can be written as:

$$\omega - \beta v_z - s\,\omega_c / \gamma = 0. \tag{1.6}$$

The equation (1.6) is the beam-mode dispersion equation.

1.2.1b Waveguide-mode dispersion relation

Waveguide-mode dispersion relation can be determined by considering a TE_{mn} mode propagating in axial direction (z-direction) of a cylindrical waveguide. For TE_{mn} mode, z-component of electric field intensity would be zero, i.e., $E_z = 0$. The axial component of magnetic field intensity in the cylindrical waveguide can be given by [Liao (1988), Kartikeyan *et al*. (2004)]:

$$H_z = C_{mn}\, J_m(\gamma_n\, r) \exp\left\{ j(\omega t - \beta z - m\theta) \right\} \quad . \tag{1.7}$$

Here, r, θ, z are cylindrical coordinates, m and n are the azimuthal and radial index of a mode, γ_n is the radial phase propagation constant, J_m is the m^{th} order ordinary Bessel function of first kind. Field constant (C_{mn}) can be given by

$$C_{mn} = \frac{1}{J_m\left(v_{mn}\right)\sqrt{\pi\left(v_{mn}^2 - m^2\right)}} \tag{1.8}$$

and

$$\gamma_n = \left(k_0^2 - \beta^2\right)^{1/2} = \left(\omega^2 / c^2 - \beta^2\right)^{1/2} = \chi_{mn} / r_w \ , \tag{1.9}$$

where, $k_0 = \omega\left(\mu_0\, \varepsilon_0\right)^{1/2} = \omega / c$ is the free-space propagation constant; c is velocity of light in free space, μ_0 and ε_0 are permeability and permittivity of the vacuum, respectively. Now, considering the axial magnetic field intensity H_{z0} at axis of the guide, i.e., r = 0. For the azimuthally symmetric mode ($m=0$), $J_0(0)=1$. Consequently,

$$H_z\big|_{r=0} = C_{mn} = H_{zo}\,. \tag{1.10}$$

Therefore, (1.7) can be written as

$$H_z = H_{z0} J_m(\gamma_n r)\exp\{j(\omega t - \beta z - m\theta)\} \quad . \tag{1.11}$$

The azimuthal components of electrical field can be written as

$$E_\theta = \left(\frac{j\,\omega\,\mu_0}{\gamma_n}\right) H_{z0}\, J'_m(\gamma_n\, r)\ \exp j\left(\omega t - \beta\, z - m\,\theta\right) \quad . \tag{1.12}$$

For the perfectly conducting waveguide wall, the azimuthal component of electric field intensity would be zero at the wall ($r = r_W$) , i. e., $E_\theta(r = r_W) = 0$. Consequently, Bessel derivative must be zero. Hence,

$$J'_m(\gamma_n\, r) = 0\,. \tag{1.13}$$

This yields

$$\Rightarrow \qquad \omega^2 - \beta^2 c^2 - \omega_{cut}^2 = 0 \quad , \tag{1.14}$$

here, $\omega_{cut} = \gamma_n c$. Equation (1.14) represents the waveguide mode dispersion plot which is a hyperbola. The intersection of the beam mode line and waveguide mode curve described by (1.6) and (1.14) provide the synchronism condition. These dispersion relations for the various gyro devices are given in Fig. 1.2 which provides the information about their operating conditions.

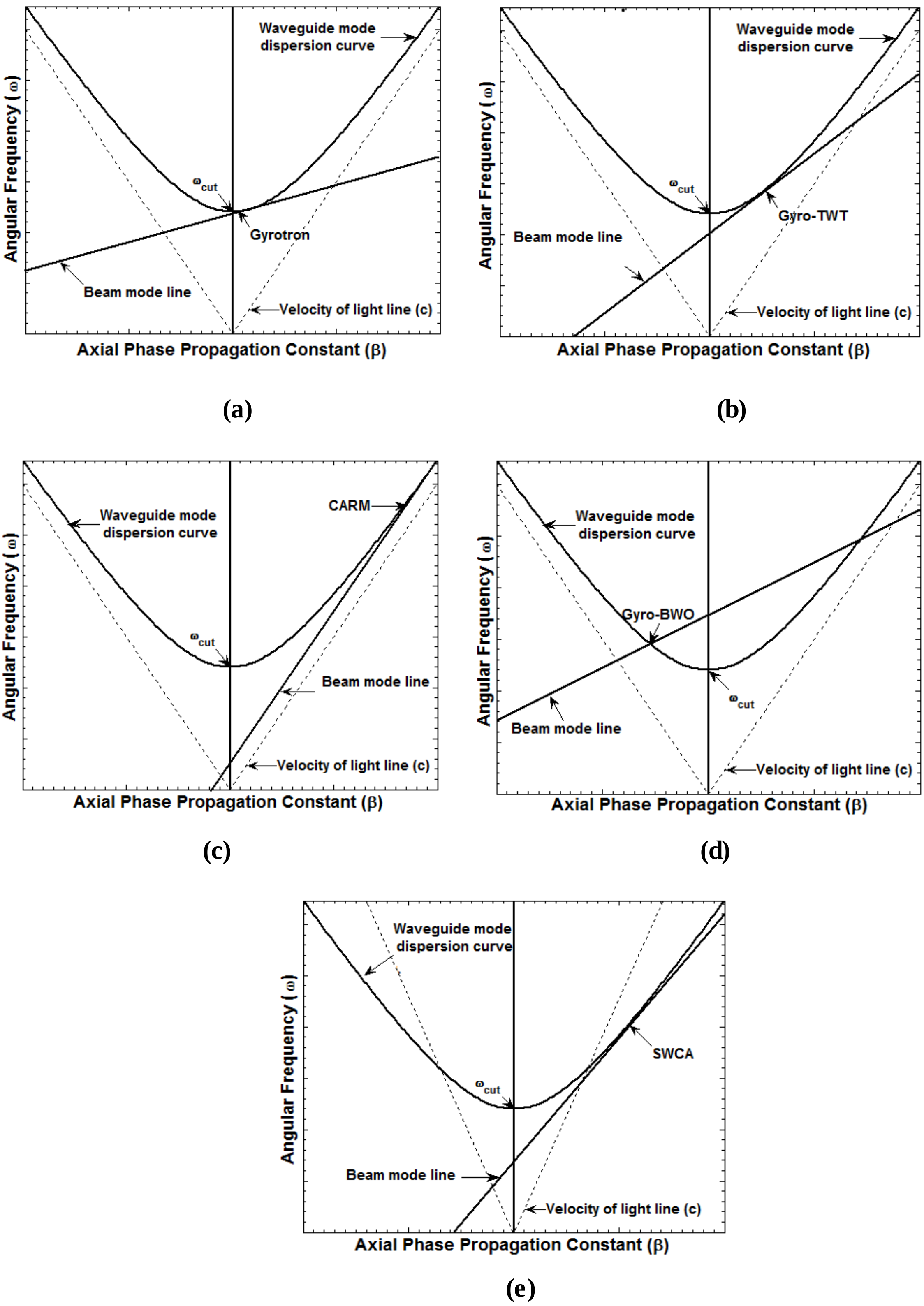

Figure 1.2: Dispersion diagrams showing the operating regions of interaction for **(a)** gyrotron, **(b)** gyro-TWT, **(c)** CARM, **(d)** gyro-BWO, and **(e)** SWCA.

In Fig. 1.2(a), the beam mode and waveguide mode dispersion relation for the gyrotron oscillators are given. Gyrotrons operate close to the waveguide cut-off frequency, at near-zero group velocity. This makes the beam velocity slow enough to maintain electromagnetic energy in the waveguide resonator cavity for interaction with the electron beam [Basu (1996), Gilmour (1986), Jain *et al.* (1994), Kartikeyan *et al.* (2004)], Symons *et al.* (1986)].

In a gyro-TWT amplifier, the grazing situation between the two curves provides the operating bandwidth of the device (Fig. 1.2 (b)). The broadband operation of gyro-TWT is desirable for the various applications that can be achieved by tuning the DC axial magnetic field to the value of grazing magnetic field. At the grazing condition, the group velocity of the beam mode and RF wave are identical that results in a high gain amplifier [Agrawal *et al.* (2001), Basu (1996), Chu *et al.* (1988), Ferguson *et al.* (1981)].

The CARM has attracted interest due to its potential for high efficiency operation, resulting from the further extended operating region of interaction where the resonance between the beam and wave is automatically maintained (Fig 1.2**(e)**). This favourable frequency shift from the cut-off frequency is caused by a large Doppler shift term associated with the large axial wave number and axial velocity [Bratman *et al.* (1981), Pendergast *et al.* (1988), Petelin (1974), Wang *et al.* (1991)].

The gyro-BWO operates at a point where both the phase and group velocities of the RF waves contain negative values (Fig 1.2(d)). By controlling either the DC axial magnetic field or the DC beam voltage, frequency tuning over a wide range of operating frequencies can be achieved in the gyro-BWO [Park *et al.* (1984), Nusinovich *et al.* (1996)].

In a slow wave cyclotron amplifier (SWCA), the axial non-relativistic bunching takes place. Additionally, the slow waveguide-mode is destabilized in such a way that the waveguide-mode dispersion characteristics is depressed below the beam-mode dispersion characteristics (Fig. 1.2**(e)**) [Baird *et al.* (1980), Choe *et al.* (1982), Ganguly *et al.* (1990)].

1.2.2 CRM interaction mechanism

The instabilities in a beam-wave system can be of different types. Their operation is mainly explained the interaction between slow and fast space charge waves on the electron beam and the electromagnetic waves in an interaction structure. The process of energy extraction is distinctive in all instabilities. The energy is extracted from the longitudinal component of the electron velocity in Cherenkov interaction [Pierce (1965)]. The interaction between a gyrating electron beam and an electromagnetic wave in the background of DC magnetic field leads to extraction of the transverse kinetic energy of the electrons. This interaction is known as the CRM instability [Chu (2004)] which occurs in the gyrotrons. In the CRM interaction, phase bunching of electrons occurs due to the change in relativistic mass as they lose or gain energy from the transverse electric field in the circuit. Another instability, which has the similar operating conditions to CRM interaction but inherently different, is termed as Weibel instability [Chu *et al.* (1978)]. In Weibel mechanism, phase bunching of electrons occurs due to axial movement of the electrons perpendicular to the cyclotron orbit as it occurs in SWCA (slow wave cyclotron amplifier) [Grantstein *et al.* (1987)]. Another instability, which is known as peniotron instability, differs significantly from that of CRM and Weibel instabilities. In peniotron interaction, energy is not extracted by the phase bunching process rather the drift of the electron guiding center causes the energy loss from each electron to the transverse electric field. The CRM, Weibel and peniotron instabilities do not have limited domains and hence they interact with each other under certain conditions [Basu *et al.* (1996)].

The typical arrangement of CRM interaction is revealed in Fig. 1.3. Considering an annular gyrating electron beam drifting through a waveguide immersed in a background axial static magnetic field B_0 [Kartikeyan *et al.* (2004)].

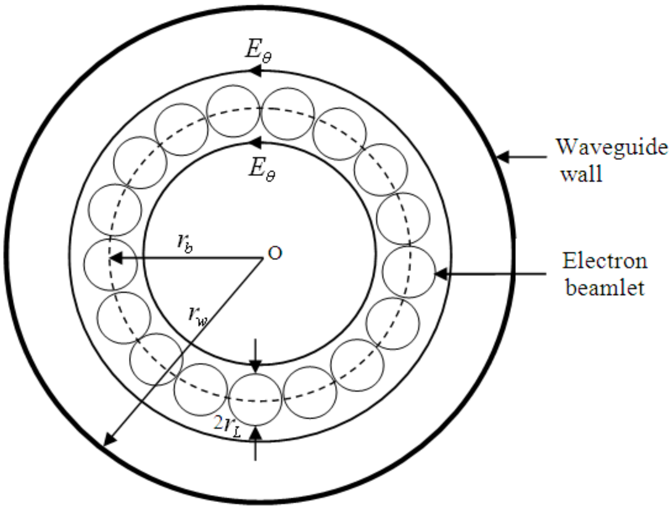

Figure 1.3: TE_{0n} mode RF electric field in a waveguide with electron beamlets.

In the figure, r_w is the radius of waveguide and r_b is the average beam radius, which is also the guiding center radius of the beamlets. The field orientation of a TE_{0n} mode is shown in the figure. The thickness of the beam is equal to twice of the Larmor radius (r_L) defined as

$$r_L = c\, v_t / \omega_c \tag{1.15}$$

where, v_t is transverse velocity of the electron, ω_c is the angular cyclotron frequency for electrons. The relativistic mass factor (γ) in terms of axial velocity (v_z) and transverse velocity (v_t) of the electron beam is as

$$\gamma = \left(1 - \left(v_t^2 + v_z^2\right) / c^2\right)^{-1/2} \quad . \tag{1.16}$$

The relativistic cyclotron frequency of the electrons can be specified as

$$\omega_c = e\,B_0 / \left(\gamma\, m_e\right) \ . \tag{1.17}$$

The azimuthal component of RF electric field (E_θ) interacts with the electrons in transverse plane. The relativistic cyclotron frequency of electrons is changed due to the alteration in the relativistic factor in this interaction. The change in cyclotron frequency established the instability that is known as Cyclotron Resonance Maser (CRM) instability. Cyclotron frequency of some electrons will increase whereas for some it decreases causing energy transfer and consequently, results in phase bunching of electrons [Chu (2004)].

1.2.2a Phase bunching

The phase bunching process can be understood easily assuming zero axial velocity. To understand this, one of the beamlets is captured to analyze the process of phase bunching as shown in Fig 1.4(a) where, B_0 is the axial DC magnetic field.

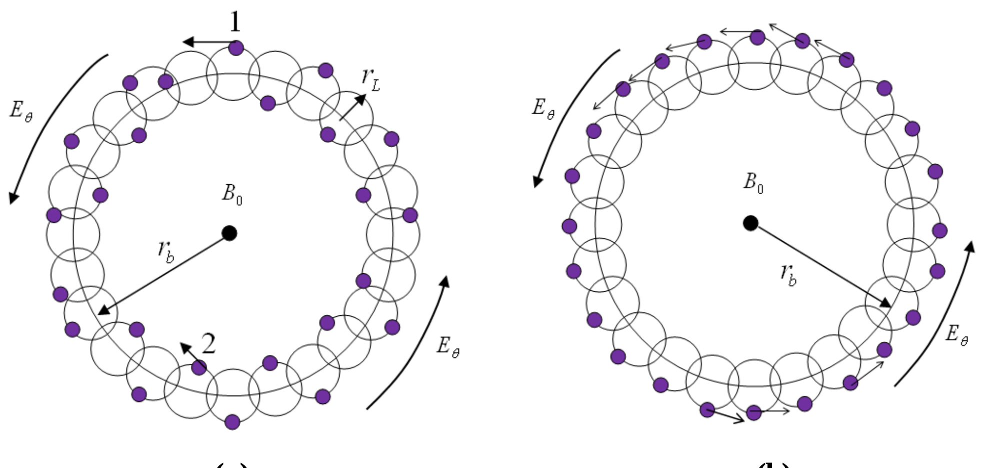

Figure 1.4: Illustration of phase bunching phenomenon in an annular electron beam **(a)** random distribution, and **(b)** phase bunched electrons in their cyclotron orbits.

The electrons are arranged in annulus circular orbits with radius r_L, typically $r_L << r_b$. From Fig. 1.4(a), initially, the phase of the electrons in their cyclotron orbits is random. The presence of a transverse RF electric field in TE_{mn} mode will cause the electrons to be accelerated or decelerated. Obviously, with the random phasing, there is no net energy exchange [Basu (1996), Chu (2004), Kartikeyan *et al.* (2004)]. Bunching mechanism can be understood by considering two electrons assigning as 1 and 2 in the Fig. 1.4(a). Due to the azimuthal electric field, electron 1 will be decelerated and lose energy whereas, electron 2 will be accelerated and hence gain an equal amount of energy. Since, the cyclotron frequency of an electron is inversely proportional to its relativistic mass γm_e (from 1.17) therefore, electrons gaining energy from the RF field gyrate slower due to increased mass while the other ones that losing energy gyrate faster due to decreased mass. As a result, the electrons form a bunch in Larmor radius. This bunch of electrons transfer energy to RF wave if the wave frequency is slightly larger than the initial value of the cyclotron frequency as

$$\omega' - \frac{eB_0}{m_e \gamma'_0} > 0 \ . \tag{1.18}$$

Here, subscript 0 refer initial value and prime denotes the reference frame in which electron axial velocity vanishes. Since, electron 2 is in the opposite direction to the electric field, energy will enhance. This causes decrease in cyclotron frequency due to increase in relativistic mass and hence, this electron moves down farther from resonance. On the other hand, electron 1, which initially loses energy, experiences an increasing value of cyclotron frequency and comes closer to exact resonance. Hence, electron 2 gaining less energy and electron 1 losing an increasing amount of energy on each successive cycle. With time, instability develops in which the wave energy grows in time and the electrons bunch in phase within their cyclotron orbits as shown in Fig. 1.4(b). Furthermore, the Larmor radii of faster gyrating electrons decreases, while those of slower gyrating electrons increases, resulting in a change in the shape of each beamlet [Chu (2004), Kartikeyan *et al.* (2004)].

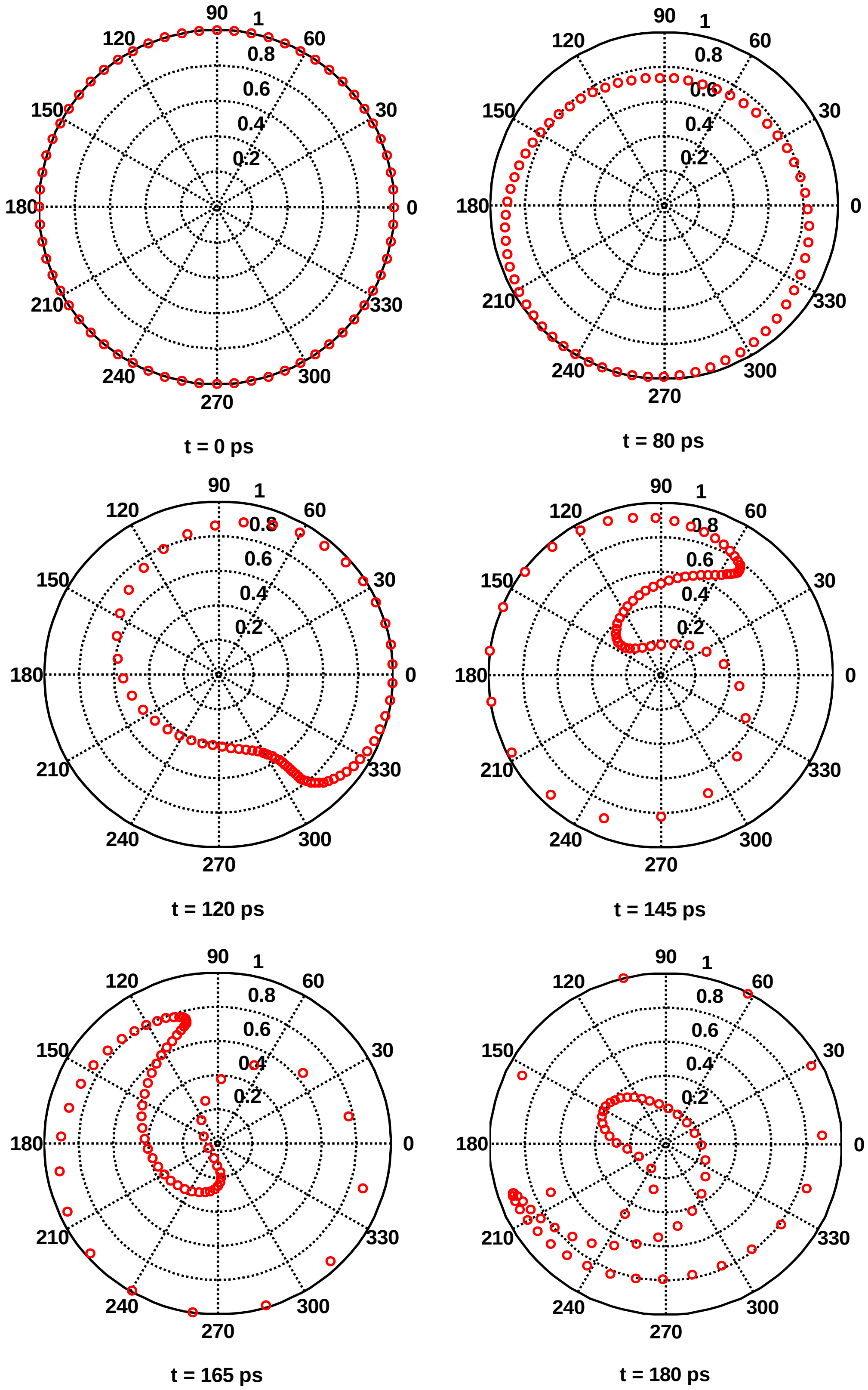

Figure 1.5: Time evolution of electrons phase distribution (shown as o) in the Larmor orbit [taken permission from Ashutosh *et al.* [2012].

The phase bunching of the electrons in CRM interaction is shown in Fig. 1.5. These figures demonstrate the Larmor radii of electrons in the phase space as a function of time. The number of representative electrons in the beamlet is taken as 64, which are initially uniformly distributed around a Larmor orbit (Fig. 1.5, at t = 0). The figures show the transverse position of electrons in the background electric field. The bunch of electrons follows the azimuthally rotating RF electric field. Obviously, Larmor radius of each electron altered and a bunch formation takes place. Finally, this bunch slips in phase to the RF and energy transfer phenomena takes place.

1.2.3 Operating principle

For the beam-wave interaction in all gyro-devices, an electron beam is emitted from a cathode and helically gyrated towards the RF interaction structure such as an open-ended cavity, series of cavities, or a long waveguide section in a background DC magnetic field. As, it has been discussed earlier that the electron beam consists of many electrons gyrating around the magnetic field lines in a small helical path with a cyclotron frequency close to the operating frequency of the device as they traverse from cathode to collector side. With such small helices, called beamlets, form a hollow annular beam in a specific beam radius. If Larmor radius of the electrons is smaller than the guiding centre radius, then device is called a small orbit device. On the other hand, if Larmor radius is greater than or equal to the guiding center radius, the device is called a large orbit device. Magnetron injection guns (MIG) are used to produce a small orbit beam. As discussed previously, the energy is extracted from the beam during the beam-wave interaction through relativistic CRM instability in gyro-devices. Bunches develop along the interaction length with time evolution. If operating frequency is slightly higher than the cyclotron frequency of the electrons, bunches slips to the phase of the

RF field and it falls in decelerating phase, consequently energy transfer takes place from beam to RF wave [Grantstein *et al.* (1987)]. In CRM interaction, the transverse energy of the electron beam is extracted to convert into RF energy. After interaction, electron beam lose its energy to the RF field in the cavity and is finally collected at a thermally cooled collector. The output RF radiations are sent through waveguides for the required application. Gyro-devices, such as, gyro-TWT, gyroklystron, gyrotwystron, gyro-BWO, and gyrotron oscillator, incorporate different types of the RF interaction structures.

1.3. Gyrotron Oscillator and its sub-assemblies

Gyrotron (gyromonotron) is an efficient high power microwave and millimeter wave coherent radiation source (oscillator) and based on CRM instability [Chu (2004)]. Gyrotron RF behavior has been extensively investigated through both theory as well as experiments in the past [Gaponov *et al.* (1981), Gilmour (1986), Grimm *et al.* (1993), Hirshfield *et al.* (1977), Kartikeyan *et al.* (2004), Kartikeyan *et al.* (2008), Kreischer *et al.* (1990), Nusinovitch (2004), Spira-Hakkarai *et al.* (1990), Thumm (2009, 2010)]. A schematic of gyrotron oscillator with axial and radial output couplings are shown in Figure. 1.6.

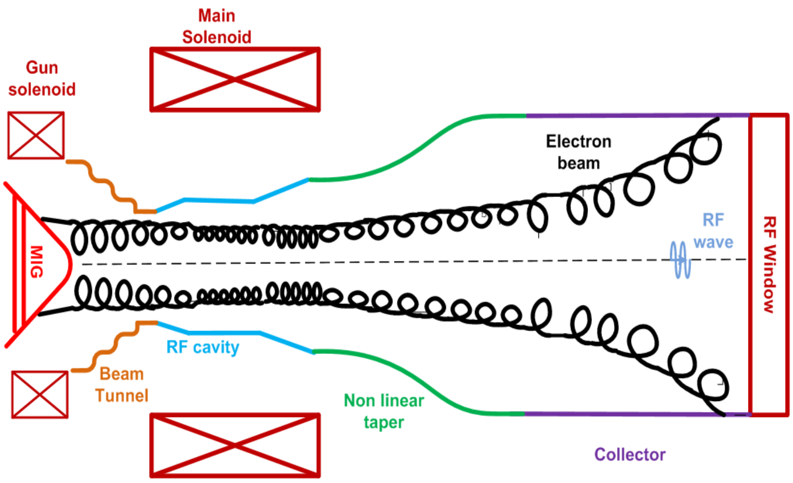

(a)

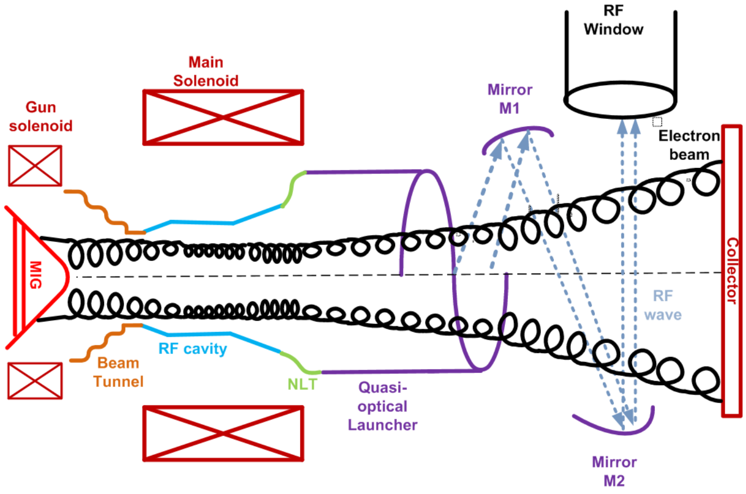

(b)

Figure. 1.6: Schematic of conventional gyrotron with (a) axial output RF coupling and (b) radial output RF coupling.

As we knew, energy has neither be created nor be destroyed, but only conversion from one form to other is possible. For this conversion, a collection of various sub-assemblies are needed. A device performance depends upon the collective performances of their sub-assemblies.

The RF source generates RF energy from a DC electron beam source with the help of a group of sub systems that allows interaction between RF wave and electron beam. For the RF source, the main goal is to convert the DC electron beam energy into RF energy with minimum losses and more efficiency. The functions of sub-assemblies of the RF device are as follows; emission and guiding of the electron beam, beam-wave interaction, and transmission of RF energy with minimum losses.

Figure. 1.6 shows the schematic diagram of the conventional tapered gyrotrons with axial and radial output RF coupling that includes its typical sub-assemblies. In the following paragraphs, the significance of various subassembly in the RF generation along with its feature are briefly described.

1.3.1 MIG gun and Beam tunnel

The source for RF generation by any microwave device is the DC electron beam. The electron beam is a bunch of electrons which are emitted from a component known as cathode in a system called as electron gun**.** The electron gun used in a gyrotron is usually magnetron injection gun (MIG) type. The conical shaped cathode emits gyrating electron beams with the electrons having small cyclotron orbits under the influence of a magnetic field, as required for the cyclotron resonance condition [Baird *et al.* (1986)].

The electrons emitted from the cathode in an electron gun of a microwave tube forms an electron beam of suitable parameters, namely, beam diameter, beam perveance, beam density, etc. and pass through the region for interaction with the RF wave. However, the beam-wave interaction in a gyrotron, the transverse electron energy is needed and thus the velocity ratio between the transverse velocity and the axial velocity is another important parameter in a function of a MIG [Baird *et al.* (1986)].

The beam tunnel is incorporated in between the electron gun and RF interaction cavity. It assists as a region where the electron beam gets stabilized. The design of the beam tunnel should be such that it should have some lossy material to absorb RF power and ensures the no backward wave propagation towards the electron gun.

1.3.2 RF interaction cavity

The RF interaction cavity mainly responsible for the generation of RF quantity with desired qualities like power and frequency, i. e., at single, step tunable and broadband frequencies. The RF waves generated in the cavity interact with gyrating electron beam emitted by MIG gun under external magnetic field. The cavity walls are made of by metals having finite conductivities. Due to this, the beam wave interaction mechanism causes ohmic losses based on the amount of RF generation in the structure which leads to thermal losses and results deformation in the cavity structure. Hence, a proper cooling system to be designed for the reliable and longer performance of the RF cavity thereby device.

Various types of the RF interaction structures, such as, tapered cylindrical cavity of simple and complex type, coaxial cylindrical cavity, photonic bandgap (PBG) type and confocal cavity type are the typically used in the millimeter and submillimeter frequency range for high power as well as low power levels. A brief discussion on the pros and cons of various interaction cavities are discussed below.

A 2-D axis symmetric model view of conventional tapered cylindrical structure view is shown in Fig. 3. It consists of three sections, first a down taper section for RF isolation of length L_d, with an angle θ_d, followed by a uniform middle section where active beam-wave interaction takes place, of length L_c and at the end, an up-taper section where RF standing waves get converted into travelling waves to extract out RF energy, of length L_u with angle θ_{up}. Usually, parabolic smoothing section of lengths L_{ds} and L_{us} at down-taper and up-taper transitions, respectively, are used to minimize the unwanted mode conversions [Edgcombe (1993)].

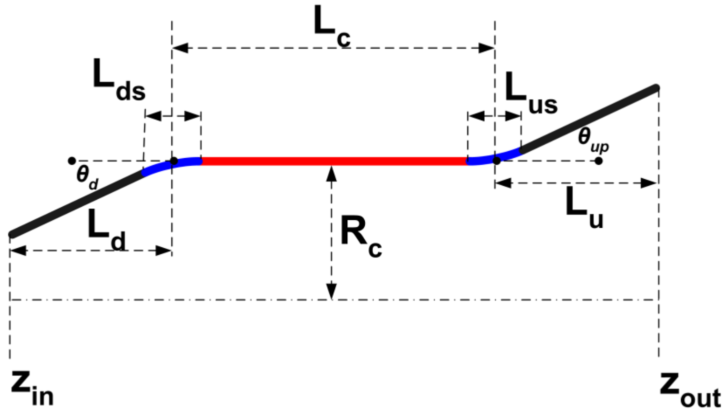

Figure 1.7: A 2D axial symmetric view of tapered cylindrical RF interation cavity.

It is fundamental, simple and conventional type of interaction cavity used for various power levels generation, i.e., all high power, medium power and low power level. Considering the high power level generation at high frequency devices, it needs to operate in the high order mode that scales the transverse dimensions as well applying high beam parameters, makes the significant presence of voltage depression also mode competition which needs a careful design of the system.

In order to ease the mode competition and voltage depression effects, coaxial resonators type cavities are being considered as the interaction structure. Basically it is a combination of tapered cylindrical cavity along with a smooth and or corrugated center conductor. A 140GHz coaxial gyrotron was experimentally demonstrated in 1999 at MIT Dammertz *et al.* (2005), and researchers at FZK are planning to use a coaxial cavity for a 2 MW, 170 GHz gyrotron [Thumm (2004)]. Apart from the lesser mode competition, considering the practical aspects, it is somewhat challenging to maintain an off beam optical axis. Beam misalignment with the cavity axis is significant in these structures that lead to degradation of the performance of the system. A careful design and machining techniques are required. Photonic Band Gap based interaction cavity, is a novel methods for mode suppression in gyrotron oscillators and amplifiers are being investigated at MIT. A photonic bandgap (PBG) structure consisting of an array of metallic rods has been successfully demonstrated in a 140 GHz gyrotron experiment [Kartikeyan *et al.* (2004)]. Even though it supports selected modes but allows more tunable bandwidth.

Confocal waveguide, a type of quasi-optical open waveguide, performs a much lower mode density than conventional cylindrical waveguide, so that it could be stably operated at high-order mode with high frequency and high power. The confocal cavity utilized in gyrotron was initially proposed by R. J. Temkin *et al.* , Lindsay (1981), and it has been successfully used in 140-GHz fundamental gyrotron oscillator and traveling wave amplifier in MIT [Lindsay (1981), Lindsay (1981), Gaponov *et al.* (1975), Flyagin *et al.* (1977)]. Due to the good mode-selective characteristics, confocal waveguide would greatly suppress the mode competition in harmonic gyrotron. A 140 GHz gyro-TWT amplifier using an open-edged confocal cavity to suppress competeing modes has also been recently tested [Barker *et al.* (2005)]. Complex cavities, formed by a group of cylindrical tapered sections and the generation of RF power achieved by operating in two different modes.

1.3.3 Non -linear taper section

A short waveguide propagating section that acts as a connecting module between RF interaction cavity and collector for axial output coupling, or the QOM converter for radial output coupling device and allows RF transmission with minimum mode conversion by providing the proper impedance matching between them. It should allow the transmission of generated RF power with minimum mode conversion from the RF cavity end to the collector end which is at different radii thereby matching different impedances. Various taper designs such as exponential taper, triangular taper, Chebyshev taper, Klopfenstein taper, and Hecken taper can be employed for matching purposes. Flügel and Kühn considered modified Dolph-Chebychev tapers for the analysis and design of circular waveguide tapers [Thumm and Kasparek (2002), Edgcombe (1993), Benford and Swegel (19920, Kartikeyan *et al.* (2004), Barker *et al.* (2005)]. Out of all, a raised cosine type taper where a uniform profile at the start and end of the taper and a non-uniform type middle profile provide better agreement with short length. Ideally, the transmission coefficient of the taper should be maximum and the reflection coefficient should be minimum with low insertion loss [Edgcombe (1993), Lawson *et al.* 1990, Goldstein *et al.* 1984].

Usually, by scattering matrix calculations, the nonlinear tapers used in the gyro devices are designed and optimized. CASCADE tool is also used for the analysis and design of the nonlinear taper. Various Optimization techniques, like, genetic algorithm

(GA), swarm optimizations, etc. are widely used for the optimization of the taper profile that leads maximum transmissions while minimum mode conversions among various modes.

1.3.4 Quasi optical mode converter

A quasioptical mode (QOM) converter, is a combination of a mode launcher, a waveguide section with a cut at its end followed by a group of beam shaping and focusing mirrors, and is incorporated in between nonlinear taper and the collector of the device to allow the conversion of cavity interaction mode TE_{mn} into a free space Gaussian beam mode TEM_{00} that low loss transmission. Incorporation of QOM converter allows separation of electron beam from the RF wave after interaction, i. e., radial output coupling and improves the overall efficiency of the devic**e** [Vlasov *et al.* (1975), Denisov *et al.* (1992), Edgcombe *et al.* (19993), Kartikeyan *et al.* (2004)]. Usually, commercially available software, such as, LOT and SURF 3D tools are popularly used for the design and optimization of QOM converters [Calcabazas creek reseach, CA] and are very much expensive for the educational institutions. There are basically two types of quasi optical mode converters are used, namely, Vlasov type and Denisov type converter. Denisov converter is a modified Vlasov converter due to improvements in the launcher structure as well improvement in the conversions efficiency [Thumm and Kasparek (2002), Edgcombe (1993), Benford and Swegel (1992), Kartikeyan *et al.* (2004), Barker *et al.* (2005)].

1.3.5. Collector

After the transfer of the kinetic transverse energy to the RF signal through effective power growth in the RF interaction structure, the spent gyrating electron beam collides at the collector and safely dissipates the remaining beam energy. In addition, the collected beam power can feed to the system as a power supply thereby enhancement in the efficiency. The overall device efficiency can be increased by incorporating depressed collector techniques, and is more suitable in the radial output couplings gyro devices. In addition, thermal studies of the collector are also important to analyze and optimize the collector efficiency as well as reliability of the system through proper cooling system design [Thumm and Kasparek (2002), Edgcombe (1993), Benford and Swegel (1992), Kartikeyan *et al.* (2004), Barker *et al.* (2005)].

1.3.6. RF window

An RF window is another crucial subassembly of the gyrotron, which ensures maximum transmission of internal generated RF power to the outer transmission. It provides a vacuum sealing between two pressure differences, typically the two pressures are 1 atm and 10^{-9} mbar (the ultra-high vacuum inside the gyrotron envelope) with low insertion loss. It should also have the capabilities of handling high peak/average power, and therefore the window material need to have high thermal conductivity and low RF loss tangent. In addition, for broadband applications, the impedance matching with rest of the RF transmission line is needed over a wideband frequencies. The desired features of an ideal RF window are as follows: low insertion loss, low reflection, wide bandwidth, high power handling, high mechanical strength, low loss tangent, i. e., low RF power absorption [Thumm and Kasparek (2002), Edgcombe (1993), Benford and Swegel (1992), Kartikeyan *et al.* (2004), Barker *et al.* (2005)].

Single disc, double disc, Brewster window, chemical vapor deposited diamond windows are the different variants of the RF window used in various fixed, high power, tunable gyrotron devices. Boron Nitride (BN), Silicon Nitride composite, diamond, Sapphire, Beryllia, Cryogenic Sapphire, Au-doped silicon and so on are the most used window materials for the gyro devices. The recent use of CVD (chemical vapor deposition) diamond RF window has significantly increased the RF output power capability of gyrotrons [30]. The Brewster windows are usually preferred for high power multi frequency operated devices as well tunable gyrotrons [Thumm and Kasparek (2002), Edgcombe (1993), Benford and Swegel (19920, Kartikeyan *et al.* (2004), Barker *et al.* (2005)].

1.3.7 External DC magnetic field

In the gyro-devices, the generation of RF with desired quantities, i.e., power and frequency in the device is attained by providing a synchronous condition between the electron beam and the RF wave in the interaction cavity. This is accomplished by the tailoring of external axial DC magnetic field profile B (z) along the device with the peak at the interaction region. The values of B (z) are primarily depending on the targeted RF frequency, *f* and *s* harmonic operation of the device [Edgcombe (1993), Kartikeyan *et al.* (2004), Barker *et al.* (2005)].

In addition to RF generation, the propagation and the guiding of the spent beam to collector and transmission of the generated RF wave is depended by the magnetic profile. The gyration of annular electron beam emitted from the MIG gun, is achieved by use of an external magnetic field and that leads the electron to oscillate with the cyclotron frequency. A tapered magnetic field, from the MIG gun to the collector with peak at the interaction cavity is maintained for guiding the electron beam and controlling the interaction with the RF wave. Cryogenic magnets, super conducting magnets as well permanent magnets are used for the facilitation of external magnetic fields required by the gyrotron. By allowing the operation of the device at second or higher harmonic frequencies, a less magnetic field is used that allows the usage of permanent magnet instead of bulky super conducting magnet with the cost of efficiency of the device [Thumm and Kasparek (2002), Edgcombe (1993), Benford and Swegel (19920, Kartikeyan *et al.* (2004), Barker *et al.* (2005)].

1.4. Applications

Gyrotron oscillators are capable of generating CW, long pulse and pulse power from few watts to few megawatts in the frequency range of millimeter, sub millimeter and THz wave at single, step tunable as well as broadband frequencies, respectively. Based on the range of power levels as well as operating frequencies and tunable frequency bands, gyrotron oscillators are suitable to use in several applications, like, plasma fusion, material processing, industrial heating, spectroscopic, medical sciences, communications (at the atmospheric window) and security application, like, in active denial systems, electronic warfare systems.

Since the ability of gyrotron to generate various ranges of CW and Pulse power at single, step tunable and continuous tunable frequencies makes its suable for use in wide variety of systems applications. A brief note on some of the areas where gyrotrons are used as the potential RF sources discussed as follows.

1.4.1 Plasma heating for fusion

The radio frequency electromagnetic waves are used for plasma heating. One kind of plasma heating method is Electron Cyclotron Resonance Heating (ECRH) which requires the sources in the frequency range of 100-200 GHz. At present, gyrotron oscillators are successively used as high power sources for ECRH applications and for plasma diagnosis of magnetically confined plasmas in controlled thermonuclear fusion research. The latest and ambitious international joint effort in the field of energy production by the controlled nuclear fusion is started in the form of ITER project with an aim to solve the problem of future energy generation to a great extent. ITER is the biggest plasma fusion machine under construction. 170 GHz gyrotron with 1 MW of output power would be used in the ITER for ECRH and ECDD (Electron Cyclotron Current Drive). High efficiency, high output power and long pulse width are the key requirements for the development of fusion gyrotrons [Kumar *et al.* (2011), Gaponov *et al.* (1994), Kasugai *et al.* (2008)].

1.4.2 Industrial heating

Development of the gyrotrons exposes new possibilities of the potential technologies for industrial material processing [Edgcombe (1993)]. Microwave or millimeter wave heating is a kind of dielectric heating in which the radiations between the frequencies ranges from 300 MHz to 300 GHz are used [Kumar *et al.* (2012)]. The utilization of microwave has been taken on in the numerous industrial heating applications, like, rubber technology, ceramic sintering, chemical processing, composite fabrication, food processing, etc. In addition to the heating and sintering of the ceramics, the millimeter wave heating is used for surface hardening, drying, removal of the organic binders and moistures from the surface, growth of nanostructure ceramics, etc. [Idehara *et al.* (2006), Abe *et al.* (2005)]. Mostly gyrotrons of the frequency range 20 GHz to 35 GHz are used in the millimeter wave industrial applications [Bykov *et al.* (2004), Litvak *et al.* (2012)]. Microwave heating mechanism energy coupling directly depends on the frequency of the radiation. By taking this aspect into consideration, the low frequency gyrotrons are suitable for heating purpose.

1.4.3 Communication, Security and atmospheric science

The presence of narrow frequency band of atmospheric windows centered at 35 GHz and 95 GHz motivates the design and development of various RF sources used in the (millimeter wave radar) communication, security and the detection applications [Kumar *et al.* (2011), Liebe *et al.* (1989)]. The advantage of having small skin depth at

95 GHz frequency compared to the other commercial microwave frequencies like 2.45 GHz or 915 MHz [Kumar *et al.* (2012)], allows design RF source based active denial system (ADS) for security applications.

The radiation can reach upto 1/64th inch in the human skin and create burning sensation. The blood vessels and nerve system are located beneath this skin depth and thus the radiation is not harmful. An Active Denial System (ADS) developed by Raytheon for the US Air Force Research Labs is a non-lethal, counter-personnel, directed energy weapon system which can be used against human targets at a distance beyond the effective range of small arms. The ADS launches a focused millimeter wave energy beam which induces unbearable heating sensation on an challenger's skin so that individual might be resisted without injury [Bratman *et al.* (2009), Kumar *et al.* (2012), LeVine *et al.* (2009)]. 95 GHz millimeter-wave radiation in the ADS also helps because of the natural atmospheric window at this frequency causing less atmospheric attenuation [Liebe *et al.* (2009), Neilson *et al.* (2009)]. This system can focus the 95 GHz millimeter wave effectually upto few kilometers. The 95 GHz gyrotron with the output power of 100 kW or more is an effective source of millimeter wave for ADS system [Hermitte *et al.* (1988)]. The radiation is non-ionizing and has small photonic energy to affect the cellular structure. Though, 95 GHz radiation creates some harmful effect on human eyes [Baird *et al.* (1986)]. The heating sensation of 95 GHz is intense but not burning because the heating sensation ends when the exposure to the radiation ends.

The facility of generation of high power at millimeter wave sources open the technological possibilities for the various kinds of atmospheric diagnosis such as measurement of humidity, turbulence structure determination, cloud monitoring, etc. 94

GHz radar system is used in the atmospheric diagnosis because of the natural atmospheric propagation window at this frequency [Mead *et al.* (1994)].

It was suggested by Manheimer Braz *et al.* (1997) that the gyrotron oscillator of 183 GHz can be effectively used in humidity detection because the water absorption rate is maximum at this frequency. The air turbulence is the major cause of air accidents. The radar system of 35 GHz as well as 94 GHz frequency can be used for air turbulence detection. The use of high power millimeter wave has also been proposed for the ozone conservation by the Wong *et al.* [Liao (2001)] and Askaryan *et al.* [Singh *et al.* (1998)]. The millimeter wave energy is capable to break the C-X bond, where X is the halogen in the upper part of the atmosphere. To paint the whole sky by the millimeter wave, thousands of gigawatt of RF energy would be required and thus hundreds of antenna station would be built on the earth. This is very expensive and huge geo-engineering project and still in research proposals.

1.4.4 Spectroscopy and medical science

One of the most significant properties of THz radiation also called submillimeter wave radiation (300 GHz to 3 THz) is its penetration through the several kinds of non-polar and non-conducting materials, like, papers, cloth, wood, etc. and can be used in the security systems [Litvak *et al.* (2012), Hornstein *et al.* (2005), Kartikeyan *et al.* (2007)]. The THz frequency fall in the spectral range of subatomic particle (like, electron spin system) and useful to characterize the materials via subatomic particles resonance [Bratman *et al.* (2009), Idehara *et al.* (2008)]. It is non-ionizing radiation (due to small energy of photon) and does not damage the tissues and DNA unlike X-ray. THz radiation shows unique spectral properties for several materials and used in the form of time domain spectroscopy [Bratman *et al.* (2009)]. In the medical science and structural biology, a THz radiation source emerged as a key component in the form of DNP /

NMR / ESR spectroscopy [Bratman *et al.* (2009), Kumar *et al.* (2011), Tatsukawa *et al.* (2005)]. The major areas of applications of THz gyrotrons are ESR and solid state NMR spectroscopy [Mehdi *et al.* (2004)].

Rather than the applications discussed above, the gyrotron is being explored for use in various new applications on the laboratory scale. Japanese groups are using gyrotron as a high power sources in the microwave rocket experiments [Piosczyk *et al.* (1996)]. G.S. Nusinovich has reported the radioactive material detection by using the THz gyrotron [Litvak *et al.* (2011)]. Gyrotrons are emerging as novel devices in various applications requiring high power RF sources.

1.5. Motivation and Objective

Observing the several advantages and emerging applications of the gyrotron oscillators over conventional microwave sources (i. e., slow-wave microwave tubes) as well as the possibilities of the stable high-power RF radiation in the millimetre and sub-millimetre wave regime, we focussed to pursue the our research in the gyrotron area. Considering the crucial role of gyrotrons in the area of, security domain as well as the spectroscopies, in the present work, we investigated the design studies of the gyrotrons that generates medium power level as well low power in the fixed and tunable frequency, respectively.

In addition, witnessing various advantages of radial output couplings of gyrotrons, like, enhancement of overall efficiency of the device, generation of practical low-loss Gaussian-like output beam modes and elimination of the long transmission line system; the design and analysis of the QOM launchers are also kept in the present research interest.

Since, the radiation of the RF energy results from the electron-beam and RF-wave interaction process which takes place in the interaction structure of the device which is a tapered cylindrical metallic cavity region. Due to finite electrical conductivity of the metallic walls of the cavity, there is ohmic losses that leads to thermo-mechanical effects on the cavity stricture and often cause structure deformations, if due care is not taken in its design. Since, the RF radiation is highly depends on cavity geometrical parameter and such ohmic losses will lead to degradation of the RF performance as well as shift in oscillation of the device. Hence its needs proper thermo-mechanical investigation and to mitigate the thermal issues, as required, an optimized cooling system has to be designed. Hence, the study of thermo-mechanical effects due to the RF power generation as well design of the optimized thermal system is essential to investigate for the gyrotron oscillators.

After the successful generation of RF power inside the device, its post-cavity subassembly, NLT section as well as the QOM launcher and RF Window transmit this RF power to the external RF transmission line. To achieve this process with minimum mode conversion and low attenuation losses; it is necessary to properly design and analyze performance of these components.

Time dependent multimode nonlinear analysis, as reported by Fliflet *et al.* (1991), is a widely accepted theory for observing the temporal growth of the RF power in the presence of various modes in the uniform section of the cylindrical cavity structure of gyrotrons. But, to guarantee the stable operation of the device, the after-cavity interactions are also need to observed. As well as the beam wave interactions under practical device considerations, like, velocity spread and the beam misalignments in the beam axis has not been explored using Fliflet *et al.* (1991) as of our knowledge.

The design of the nonlinear taper (NLT) section can be confirmed with the help of scattering matrix analysis in the structure by calculating the transmission and reflection coefficients versus frequency of the interaction cavity modes. A Commercially available CASCADE tool has been used for this purpose in general In addition, due to the irregularities in the dimpled mode launchers, the main interaction mode coming from the cavity is coupled to several modes and the optimized dimpled launcher results a Gaussian beam like mode on the launcher cut with a Gaussian content factor (GCF) of more than 99%. Now a days, people are using the commercially available LOT and SURF 3D tools from Calcabazas Creek Research, CA which is an expensive for the educational purpose. Hence, design and optimization of the QOM launchers through analysis is still a challenge.

Since, the determination of probable interaction cavity dimensions are determined from the cold cavity analysis by solving the single mode Vlasov approximation. As well, the parameters are optimized through beam wave interactions with the use of Gaussian field profiles in the case of single axial mode variation. Considering these two, we can design the NLT section by inspecting the field profile at the beam absent condition through the Vlasov approximation theory and the design in confirmed by incorporating calculated field profile in the beam wave interaction studies. As well, by developing a numerical code based on the coupled mode theories and using the wave equations in the launcher domain, the study of Denisov launchers are planned to be carried out.

1.6. Plan and Scope

Gyrotron oscillator is a well-established compact, stable and efficient fast-wave device, radiating high-power in the millimetre and sub millimetre frequency regime and have numerous potential applications. In the present dissertation, its design methodology and analytical & simulation investigations of the single frequency as well as tunable frequency gyrotrons are planned to be carried out. Design studies of the gyrotrons using tapered cylindrical cavity type RF interaction structures operating for the single frequency, generating medium power level gyrotrons, operating in whispering gallery mode and volumetric mode are investigated. The device design methodology, RF and beam parameter selection, electron-beam and RF-wave interaction behaviour as well as thermo-mechanical performance are to be studied through rigorous analysis and to be verified through simulation studies.

For the first time, we have used single simulation tool for the gyrotron beam wave interaction and thermal studies. We have also suggested modified device design to mitigate the thermo-mechanical effect and its effect on the device RF performance are investigated. Followed by, the design and analysis of the post interaction cavity components, like, the nonlinear taper (NLT) section, quasi optical mode (QOM) launcher and the output RF windows for transmission of the generated power in the interaction cavity to the external transmission line are described. An afetrcavity interaction study for single frequency gyrotron oscillator is also carried by considering uniform axial DC magnetic field profiles. In addition, the design and frequency tuning studies of low power, tunable frequency gyrotrons for DNP enhanced NMR spectroscopies with electrical and magnetic tunings are described. Necessary steps required for the device parameters selection, tapered cavity RF interaction structure design of the tunable frequency gyrotrons are discussed. Further, the RF window used for the tunable frequency RF extraction is also presented.

In Chapter 1, with the introduction of gyro-devices evolution and literature review of high and low power gyrotrons operating in the single frequency and tunable frequency, respectively. Operating principle, and sub-assemblies of the gyrotron oscillators are presented. Thereafter, various output couplings used in the gyrotrons and their advantages as well challenges are briefly described. The applications of various power level gyrotrons generating RF radiation at single and tunable frequency are discussed. The motivation of the present research and the organization of the thesis are drawn at the end of this chapter.

In Chapter 2, the post interaction components, i.e., quasi optical mode (QOM) converters that are responsible the radial coupling output for the device are investigated for its design and performance study. The basic theory and the design equations for the conventional Vlasov and Denisov types of QOM launcher are presented. The design parameters of the Vlasov launchers for the 95GHz, 100kW TE_{62} and $TE_{10,4}$ modes gyrotrons, a single frequency medium power level rating, to be presented in the Chapter 3 and 4 of this thesis are determined. Then observing the practical limitations and design considerations of Vlasov type converters, in the present work, Denisov type launchers are designed. A brief notes on the coupled mode theory used for the analysis of Denisov type launchers are also described. Usually, the QOM converters are designed and optimized by widely accepted commercial software's LOT and SURF3D developed Calabaza's Creek. Considering its unavailability with respect to cost with researcher, we developed our own numerical code in the Matlab domain based on the theoretical concepts. Developed code validation as well as the optimization of the Denisov's launchers for the $TE_{10,4}$, 95GHz 100kW by inspecting the mode variation profiles along the launcher section followed by wall field intensity profiles are described in this chapter. Further, the analysis and design of single disc type output RF windows for various type of operating modes, i. e., TE_{mn}, TM_{mn} and TEM_{00} are discussed followed by the design of the RF windows for the proposed structure are presented.

In Chapter 3, design methodology, analysis and simulation of a tapered cylindrical cavity 100kW gyrotron oscillator operating in $TE_{6,2}$ at 95GHz is presented. The basic theory, design constraints, methodology and the analysis used for design of fixed frequency tapered interaction cavity are described. Non-linear, time dependent, multimode theory proposed by Fliflet *et al.* [1991] are used to develop indigenous code and used for the analysis of the designed gyrotron device. By investigating the electron-beam and RF-wave interaction behaviour using this analytical code is got verified by comparing the results with those obtained through PIC simulation reconfiguring a Commercial PIC code "CST Studio Suite". The device design is further optimized at a uniform axial DC magnetic field profile. The device performance is further investigated under practical considerations, namely, velocity spread and beam misalignments. The thermo-mechanical analysis of the designed RF cavity structure is also carried out. Also, the design of an optimized cooling system is presented and the system performance got verified through simulation using "COMSOL Multiphysics" commercial code.

Considering the challenges and issues related to deformations and misalignments caused due to thermo-mechanical effect, in Chapter 4, we designed, analyzed and simulated the same rating gyrotron device (100kW, $TE_{6,2}$ mode, 95GHz) as discussed in Chapter 3 is now proposed to investigate while working at a relatively higher order mode $TE_{10,4}$- which would allow a larger transverse dimensions thereby more relaxation regarding thermal issues as well as it could also be upgraded to higher power levels too. After the RF interaction cavity structure design, to ensure stable device operation, the beam wave interaction studies of the cavity structure by adding a raised cosine type non-linear taper (NLT) is carried-out for an axial uniform DC magnetic profile. Since, the time dependent multimode analysis is used so far considering the uniform section of the cavity with ideal gaussian type field profile. In the present work, we have now extended studies till NLT end section by incorporating the actual field profiles calculated by solving the Vlasov approximation equation to the combined RF cavity and NLT geometry. The beam wave interaction studies, as well as the effect of beam misalignments on the beam coupling to the TE_{mn} mode and the effect off offset in the beam axis with respect to the cavity axis are studies. Instead of performing the thermo-mechanical behaviour simulation using a now code, COMSOL Multiphysics, for the present case, the thermo-mechanical analysis is also simulated using the same code used for beam-wave interaction simulation. For the first time we have used a single commercial code "CST Studio Suite" and its Steady state thermal solver as well Mechanical solver tool sucessfully applied for the gyrotron.

In Chapter 5, the design and analysis of low power tunable gyrotrons for the DNP enhanced NMR applications are presented. Various tuning techniques used in gyrotrons are discussed. In the present work, we have described the design methodology and designed an RF interaction structure that is able to generate a minimum RF power of 20W over a band of 2.4GHz for $TE_{5,3}$, 263GHz gyrotron for the 400MHz DNP NMR spectroscopy applications. Here also, by allowing the actual field profiles calculated for the RF interaction cavity geometry from the Vlasov approximation for the high order axial modes, the time dependent multimode analysis is carried out at several beam currents via electrical and magnetic tunings and the RF power output are described. Then considering a SiO_2, as window material, the design of single disc type RF window is also presented.

With acquired knowledge from Chapter 5, that longer integration cavities lower the start oscillation current of mode excitation as well as it also allows the excitation of high order axial modes. In Chapter 6, an experimentally demonstrated low power tunable gyrotron operating in $TE_{0,3}$ at 140 GHz, is revisited and the reported RF interaction cavity tailored such that excitation of the higher order mode via magnetic tuning leads to device frequency tunability. The enhancement in the tuning bandwidth of modified device is also demonstrated.

In the last chapter, Chapter 7, the work embodied in the present thesis are summarized and the significant conclusions are drawn from the major findings. The limitations of the present study are discussed pointing out the scope for the future work.

--- XXX ---